A METHOD TO DERIVE OPTICAL PROPERTIES OVER SHALLOW WATERS USING SEAWIFS

Chuanmin Hu, Frank Muller-Karger, Kendall L. Carder, Zhongping Lee
Department of Marine Science, University of South Florida
140 7th Ave. S., St. Petersburg, FL 33701
(727)553-1186, hu@carbon.marine.usf.edu

ABSTRACT

The current NASA SeaWiFS algorithms frequently yield large errors when used to estimate phytoplankton pigment concentrations over shallow waters. In areas where the ocean bottom intersects the first optical depth, water-leaving radiance often contains light reflected off the bottom, and thus the default NASA bio-optical algorithms cannot be used. In very shallow areas, such as the Great Bahama Bank, the total radiance received by the SeaWiFS sensor is normally higher than expected oceanic values, and these areas are masked to inhibit further processing. As a result, no atmospheric correction is carried out, and water-leaving radiance can not be obtained. In this paper, we present a method to retrieve the bio-optical properties such as pigment and dissolved organic matter (absorption), bottom depth, and bottom albedo over shallow waters. We modified the SeaWiFS processing code to avoid masking of shallow, bright waters and to retrieve the water- leaving radiance in these areas. We compared aerosol optical properties derived from SeaWiFS data over the shallow area and over adjacent deep waters to validate our approach. We find that in shallow (probably 4m or greater) clear water, the Gordon-Wang SeaWiFS atmospheric correction scheme is still robust. A semi-analytic optimization model is used to retrieve the under-water optical properties. We tested our algorithm in areas of known bottom depth and albedo (e.g., Gulf of Batabano, South of Cuba), and in areas where field data were collected (e.g., the Great Bahama Bank). Good agreement is found between the SeaWiFS-derived and validation values. Possible error sources are discussed.

Keywords: SeaWiFS, pigment, dissolved organic matter, bottom albedo, remote sensing.

INTRODUCTION

With over one year of operation since September 1997, the SeaWiFS sensor has proven with great success that it is useful to monitor ocean, land and atmosphere color. In coastal waters, where phytoplankton pigments and their degradation products are not the only optically important constituents, however, SeaWiFS generally fails in estimating water-leaving radiances and pigment concentrations. There are mainly two reasons that account for this. One, band 7 (765nm) and band 8 (865nm), which are used to determine the atmospheric contribution to the total radiance received by the sensor (Gordon and Wang 1994), are contaminated by reflective water constituents that do not co-vary with phytoplankton (e.g., suspended sediments) and/or light reflected off the bottom. Second, the default NASA bio-optical algorithms generally cannot be applied to coastal case 2 waters to estimate either pigment or DOM abundance. In previous work (Hu et al. 1998), we developed a preliminary algorithm to work on turbid coastal waters by using adjacent,

offshore atmosphere properties and a new bio-optical model. Here we present a method to derive the underwater optical properties in clear, shallow coastal waters

METHOD

Our first step is to derive remote sensing reflectance (Rrs) at the visible SeaWiFS bands (412, 443, 490, 510, 555, and 670nm) over the coastal area of interest using a modified version of the NASA software package (SEADAS). Over optically shallow water where the bottom contributes a significant portion of the total radiance (L_t), L_t at any band exceeds a certain threshold, and a mask is applied by the default algorithm and further processing is inhibited (McClain et al. 1995). Figure 1A shows the total radiance in digital counts at band 8 (865nm) over the Florida Keys, Cuba, and the Great Bahama Bank from a SeaWiFS L1A image taken on March 3, 1998. Figure 1B shows the normalized water-leaving radiance (nL_w) at 555nm retrieved from the L1A imagery using the default NASA algorithm. Coastal regions are masked even where L_t at 865nm in Figure 1A does not show any apparent contamination from the water. For example, the total reflectance, ρ_t (following Gordon and Wang, $\rho = \pi L/(F_0 \cdot \cos\theta_0)$ where L is the upward radiance, F_0 is the extraterrestrial solar irradiance, θ_0 is the solar zenith angle), at 865nm along a horizontal line (Figure 1A) across the deep-shallow water boundary is drawn in Figure 2. Except for a few pixels at the eastern end, $\rho_t 865$ is found to be fairly homogenous across the boundary and over the entire shallow bank. The same is found at 765nm. This suggests that the default NASA atmospheric correction scheme (Gordon and Wang 1994) may be applied over the area since there is no apparent contribution of bottom reflectance to total scene reflectance.

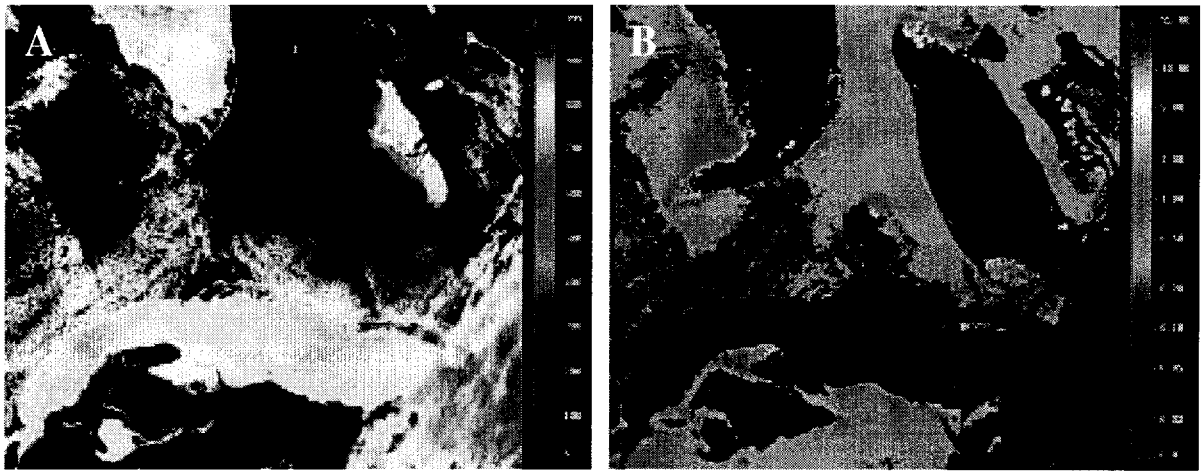

Figure 1. SeaWiFS imagery obtained with an HRPT station at the University of South Florida on March 3, 1998. A) Total radiance (in digital counts) at 865nm received by the sensor (Level 1A data); red line east of Florida Strait represents transect for data shown in Figure 2. B) Normalized water-leaving radiance (nL_w) at 555nm ($mW \cdot \mu m^{-1} \cdot cm^{-2} \cdot sr^{-1}$) obtained with the default NASA algorithm showing large masked regions (black) over the Florida Keys, Gulf of Batabano (South of Cuba), and the Great Bahama Bank. Clouds are also shown in black in this latter image.

Our approach is to remove this shallow water mask and then to proceed to compute aerosol properties and water-leaving radiances. Figure 2 shows aerosol reflectance at 865nm, ρ_a865, derived after removing this mask. Figure 3 shows normalized water-leaving radiance at 555nm and 670nm.

In Figure 3A, generated with our modified code, nL_w555 over the open ocean is identical to that in Figure 1B. It is also consistent with the value of 0.28 $mW \cdot \mu m^{-1} \cdot cm^{-2} \cdot sr^{-1}$, given by Gordon and Clark (1981) for clear water regions. Over the shallow waters, however, nL_w555 increases by a factor of 5 to 50 (see Great Bahama Bank region). Since the optical depth is so small in the visible bands, even SeaWiFS band 6 is affected; this can be seen as an increase in nL_w670 (Figure 3B).

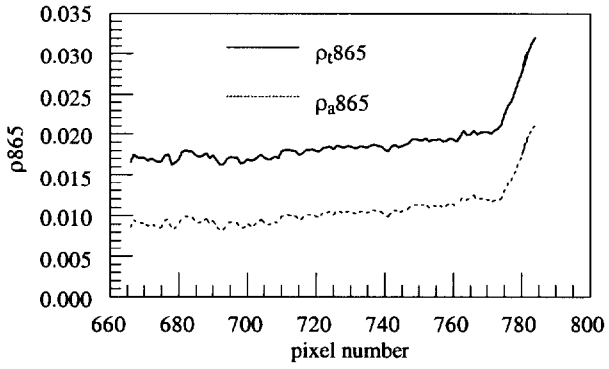

Figure 2. Total reflectance (ρ_t865) extracted from the Level 1A image (Figure 1A) and aerosol reflectance (ρ_a865) obtained from modified NASA algorithms along the transect shown in Figure 1A.

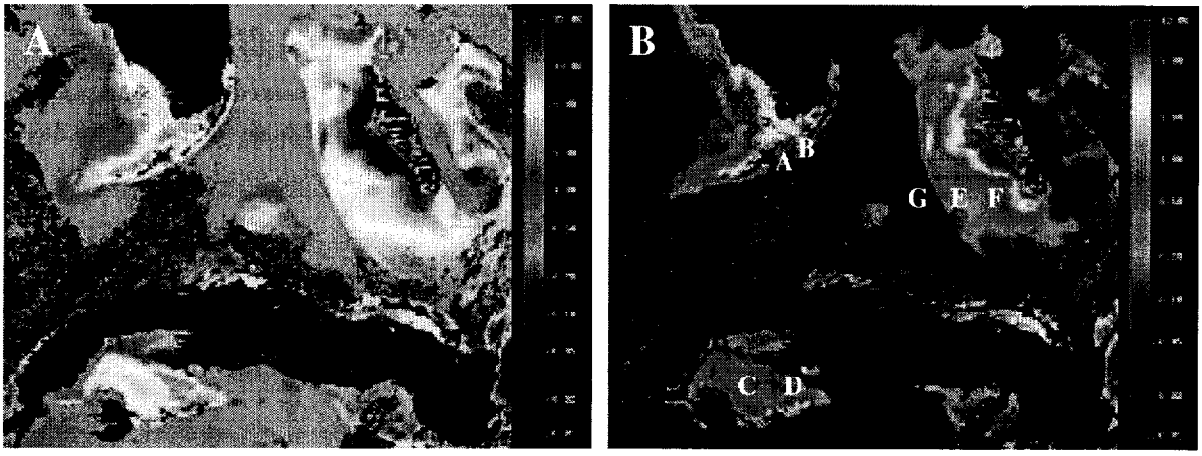

Figure 3. Normalized water-leaving radiance (nL_w) at 555nm (A) and 670nm (B) derived from SeaWiFS imagery collected on March 3, 1998 using a modified NASA algorithm (SEADAS) after turning off the shallow water mask. Over shallow regions like the Keys, Gulf of Batabano, and the Great Bahama Bank, nL_w increases by factors of 5 to 50 as compared with nL_w from the open ocean. Seven pixels are studied and their locations are marked as "A" to "G" in Figure 3B. Pixel "E", "F", and "G" are located along the transect line east of Florida Strait.

From nL_w, remote sensing reflectance, Rrs, is easily derived as $Rrs(\lambda) = nL_w(\lambda)/F_0(\lambda)$, where F_0 is the extraterrestrial solar irradiance. A semi-analytic (SA) optimization model (Lee et al., 1998) is then applied to $Rrs(\lambda)$ to derive the underwater

optical properties. In the model, some properties are assumed known and are obtained from the literature, specifically water absorption and scattering coefficients, and the DOM absorption spectral slope (we used S=0.015). There are several variables in the SA model, such as pigment absorption at 443nm ($a_\phi 443$), DOM absorption at 443nm ($a_g 443$), bottom depth (H), bottom albedo at 555nm ($B555$), etc. (Lee et al., 1998), which are tuned to minimize the RMS error between the modeled Rrs(λ) and the SeaWiFS Rrs(λ).

RESULTS

The optimization method described above is expensive computationally (~1 minute per pixel on a Pentium II/300), and therefore application of the method to an entire SeaWiFS image, or even to the large areas that we have "unmasked" is not practical at this stage. Therefore, we chose only a few points in which to run the model: within Hawk Channel (Florida Keys), the Gulf of Batabano (Cuba), and the Great Bahama Bank (see crosses in Figure 3B), where bottom depth was derived from bathymetric maps (BBA Chart Kit Region 8 1995 and Region 9 1991) and where bottom reflectance was known from recent field trips. The Rrs spectra from SeaWiFS and from the SA optimization model are presented in Figure 4. The modeled and the SeaWiFS spectra agree very well, with an RMS error <6% for each of the seven pixels. The variables derived from the SA model for the seven pixels are listed in Table 1.

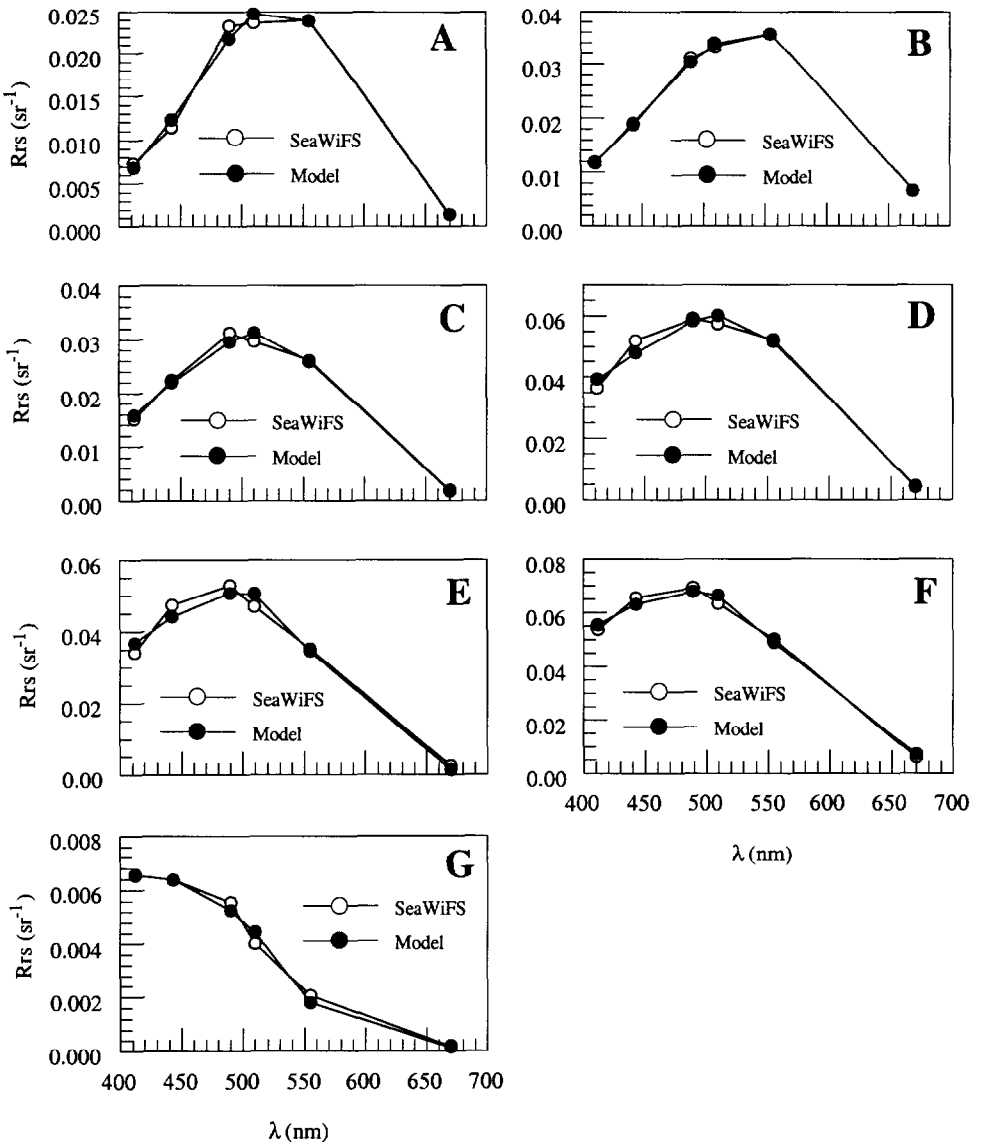

Figure 4. Spectra generated from the SA optimization model, as compared with SeaWiFS data. Panels A to G correspond to pixel labels shown in Figure 3B. The RMS error between the modeled and SeaWiFS spectra is less than 6% for all pixels.

In Table 1, $a_\phi 443$ is $0.005 m^{-1}$ at 5 of the pixels used. This value was fixed as a constraint during the optimization. If the specific absorption coefficient $a_\phi^* 440 = 0.034$ $m^2 mg^{-1}$ or higher were to be used (Gordon 1992), this would imply a pigment concentration $<0.15 mg/m^3$, which is reasonable according to field observations (Moore and Farmer, Hochman, Peacock, and Steward, personal communication). Pixels A and B are from Hawk Channel, where B is closer to shore and pigment is estimated to be $\sim 1 mg/m^3$. The DOM absorption ($a_g 443$) and bottom albedo are about the same at both places, while the modeled water depth decreases from 5.07m at A to 2.88m at B. This is confirmed by data from the bathymetry map. All derived parameters show reasonable values according to field observations, except that at pixel D, E, and F, the estimated

bottom albedo appears rather high (>50%). Recent studies near Lee Stocking Island, Bahamas have discovered albedos that high for oolites (Mazel, personal communication). To test our method, we chose pixel G from deep ocean water where the default NASA algorithms give a chlorophyll *a* concentration of 0.214mg/m^3. By limiting the depth to more than 200m, the model gives $a_\phi 443 = 0.008 m^{-1}$, which is equivalent to a concentration of 0.235mg/m^3. $a_g 443$ at pixel G is $0.0186 m^{-1}$, which is typical for clear ocean water. In general, the water depth predicted by the model over shallow waters results in errors less than 30%, while the bottom albedo tends to have higher errors.

Pixel	Lat. (°)	Lon. (°)	$a_\phi 443$ (m^{-1})	$a_g 443$ (m^{-1})	*B*555 (%)	*H* (m)	H_0 (m)
A	24.678	-81.025	0.005	0.081	30.1	5.07	6.4
B	24.705	-80.993	0.033	0.073	30.7	2.88	4.2
C	22.125	-82.104	0.005	0.0132	31.7	5.56	6.0
D	21.991	-81.890	0.005	0.0212	51.0	4.07	6.0
E	24.084	-78.753	0.005	0.0188	55.7	7.6	6.1
F	24.015	-78.271	0.005	0.056	45.0	4.84	4.0
G	24.159	-79.274	0.008	0.0186	0	> 200	> 500

Table 1. Results from the SA optimization model for the seven pixels shown in Figure 3B. $a_\phi 443$ is pigment absorption at 443nm, $a_g 443$ is DOM (or gelbstoff) absorption at 443nm, B555 is the bottom albedo at 555nm, H is the bottom depth, and H_0 is the bottom depth given by sonar bathymetry maps over the Keys and the Great Bahama Bank. Bathymetry information for the Gulf of Batabano (Cuba) was provided by N. Melo (personal communication).

Several factors cause errors in the SA optimization model. First, some parameters used in the model, such as the DOM absorption spectral slope, are estimates from previous work. Secondly, the spectral shape of the bottom reflection is generalized from previous field measurements and is predetermined in the model; this spectral shape may differ in the environments we studied. Finally, as reported in the literature, there is some degradation in the SeaWiFS bands that is not yet properly accounted for in the calibration of this sensor. Through September 1998, for example, gain settings in the default NASA algorithms were changed at least three times, and adjustments are not likely to be final. However, the relative response of gains at different bands will greatly affect model performance. For example, if we increase Rrs at band 4 (490nm) by 5% (from 0.02364 to 0.025) at pixel A, then we would have $a_\phi 443$ as $0.01 m^{-1}$, $a_g 443$ as $0.077 m^{-1}$, *B*555 as 0.50 and *H* as 6.8m. The model was initially developed using AVIRIS data; therefore lack of spectral information at SeaWiFS bands between 555 and 670nm also leads to errors in the optimization.

CONCLUDING REMARKS

SeaWiFS has unused capabilities which are relevant to coastal areas. Currently, many coastal areas are either masked or the bio-optical algorithm is not applicable. Here we presented a method to extract the data from such masked areas by carefully examining the SeaWiFS atmospheric correction bands (765 and 865nm) and applying the Gordon-

Wang (1994) atmospheric correction scheme. We derived water-leaving radiances which were further used in a semi-analytic optimization model to obtain underwater bio-optical properties. We found that chlorophyll pigment concentration, gelbstoff absorption, and water depth may be derived within reasonable errors. However, large errors occur in the estimated bottom albedos. We hope to improve the model performance by using more realistic bottom reflection spectral shapes. However, more work is needed to make use of the SA optimization model for operational processing of SeaWiFS imagery.

We thank H. Hochman, T. Peacock, R. Steward, C. Moore, C. Farmer, C. Mazel, and N. Melo for their information from the field work. This work was funded by NASA contracts NAS5-97128, NAS5-31716, NAGS-3446, and NAS-97137 and ONR contract N00014-89-J-1091 to the University of South Florida.

REFERENCES

H.R. Gordon, and M. Wang, "Retrieval of Water-Leaving Radiance and Aerosol Optical Thickness Over the Oceans with SeaWiFS: A Preliminary Algorithm", Appl. Opt., **33(3)**, 443-452 (1994).

C. Hu, K.L. Carder, and F. Muller-Karger, "Preliminary Algorithm to Derive Chlorophyll Pigment Concentration and DOM Absorption in Turbid Coastal Waters from SeaWIFS Imagery", Proceeding of The 4th Pacific Ocean Remote Sensing Conference (PORSEC'98), in process (1998).

C.R. McClain, R.H. Evans, and M. Darzi, "SeaWiFS Quality Control Masks and Flags: Initial Algorithms and Implementation Strategy, *NASA Tech. Memo." 104566,* **28**, S.B. Hooker, E.R. Firestone, and J.G. Acker Eds., NASA Goddard Space Flight Center, Greenbelt, Maryland, 38pp., plus color plates, 3-7 (1995).

H.R. Gordon, and D. Clark, "Clear Water Radiances for Atmospheric Correction of Coastal Zone Color Scanner Imagery", Appl. Opt. **20(24)**, 4175-4180 (1981).

Z. Lee, K.L. Carder, C.D. Mobley, R.G. Steward, and J.S. Patch, "Hyperspectral Remote Sensing for Shallow Waters: 2. Deriving Bottom Depths and Water Properties by Optimization", submitted to Appl. Opt. (1998).

H.R. Gordon, "Diffuse Reflectance of the Ocean: Influence of Nonuniform Phytoplankton Pigment Profile", Appl. Opt. **31**, 2116-2129 (1992).

C.A. Moore, and C. Farmer, Rosenstiel School of Marine and Atmospheric Science, University of Miami, 4600 Rickenbacker Causeway, Miami, FL33149, personal communication (1996).

H. Hochman, T. Peacock, and R. Steward, Marine Science Department, University of South Florida, 140 Seventh Avenue, S., St. Petersburg, FL 33701, personal communication (1998)

Chart Kit BBA: Florida West Coast and the Keys, Region 8 Chart Kit, Ninth Edition, Better Boating Association, Inc. (1995).

Chart Kit BBA: The Bahamas, Region 9 Chart Kit, Fourth Edition, Better Boating Association, Inc. (1995).

C.H. Mazel, Massachusetts Insitutute of Technology, Department of Ocean Engineering, 77 Massachusetts Ave., Cambridge, MA 02139, personal communication (1998).

N. Melo, Institute of Oceanology, Havana, Cuba, personal communication (1998).